

## Analytical modeling of a multi-linkage planar mechanism

Chunli Wang<sup>1</sup>, Xiulong Chen<sup>2</sup>, Yu Deng<sup>3</sup>

<sup>1-3</sup> College of mechanical and electronic engineering, Shandong University of science and technology, Qingdao, China

### Abstract

In order to realize the analytical modeling of a planar multi-linkage mechanism, a six-bar linkage planar mechanism is taken as an example, the kinematic model of the six-bar linkage mechanism is established by complex number vector method, the dynamic model is established by Lagrange Method, the kinematic state and force state of mechanism are analyzed. Firstly, the model of displacement, velocity and acceleration of the six-bar mechanism are deduced by resolution method. Secondly, the dynamic model of six-bar mechanism is established by Lagrange Method. Finally, combined with examples, numerical verification and virtual simulation verification of the results of slider position, slider velocity, slider acceleration, and driving torque are all carried out. The research can not only provide theoretical basis for analytical modeling and solution of kinematic analysis, force analysis and structure design of the six-bar mechanism, but also suggest a way of thinking about analytical modeling for other multi-link mechanism.

**Keywords:** multi-linkage planar mechanism, kinematic analysis, lagrange method, dynamics

### 1. Introduction

Compared with the slider-crank mechanism, the multi-link mechanism has the advantages of high controllability, high precision, high efficiency, low noise, small vibration, long service life, energy saving and environmental protection. The multi-link mechanism can realize the forming technology that the slider-crank mechanism cannot achieve, and meet the requirements of a variety of stamping operation. Therefore, now the multi-link mechanism has received much attention from industrial circle and scholars [1-3].

The kinematics and forces analysis of multi-link mechanism, which is the foundation of study on stiffness and control system design [4-5], provides an important theoretical basis for structure design of the mechanism. Up to now, domestic and overseas scholars have done a large number of researches on multi-link mechanism and achieved a series of research results in these areas [6-20], such as the configuration selection, mechanism design, forming technology, task characteristics and virtual prototype simulation. However, there have been few efforts made oriented to analytical modeling which contains kinematic model, kinetostatics model and dynamic model at the same time. Then the kinematic and force analysis have not been sufficiently considered. To meet the needs of the analysis and design of the modern high precision multi-link mechanism and promote its development and application, there is an urgent task to carry out the research on analytical modeling. This paper takes a six-bar mechanism as an example, the analytical models of the mechanism are established, and kinematics and force analysis of the mechanism is carried out. By numerical computation and virtual prototype simulation, the correctness of the analytical models is verified.

### 2. Kinematics model of the six-bar planar mechanism

#### 2.1 Architectural feature of the six-bar mechanism

As shown in figure 1, this six-bar mechanism includes a

frame 1, a crank 2, a linkage 3, a rocking-bar 4, a linkage 5 and a slider 6. The crank 2 and the rocking-bar 4 are respectively connected with a machine frame through a revolute joint, crank 2 is connected with servo motor and driven by the motor, the linkage 3 is connected with the crank 2 through a revolute joint, linkage 3, rocking-bar 4 and linkage 5 are connected in the same place by revolute joints, the end of the linkage 5 is connected with the slider 6 through a revolute joint, the slider 6 is in the fixed guide rail, so the slider 6 can move only in the vertical direction. This six-bar mechanism, which can be used as a press machine for large-scale industrial production or a teaching press prototype, is developed by our laboratory. The degree of freedom of the mechanism is 1, and the motion of the mechanism can be driven by the crank 2. The structure chart of six-link mechanical press is shown in figure 2.

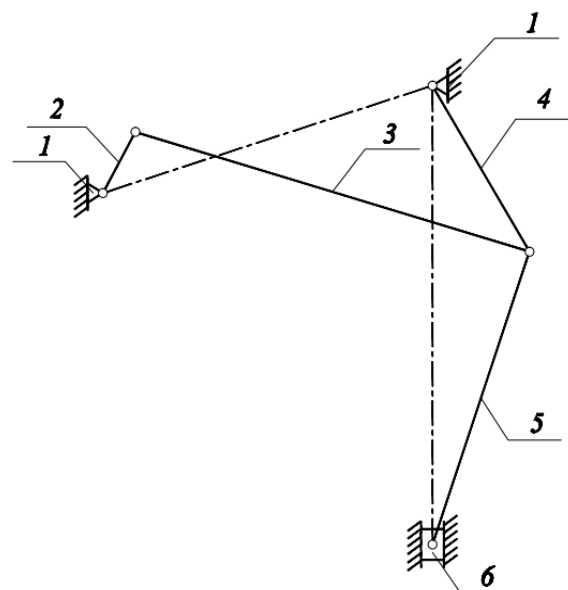


Fig 1: Schematic diagram of six-bar mechanism

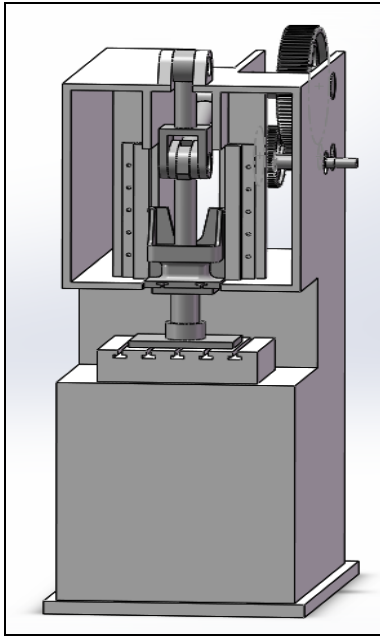


Fig 2: Structure chart of six-link mechanical press

## 2.2 Displacement model of the mechanism

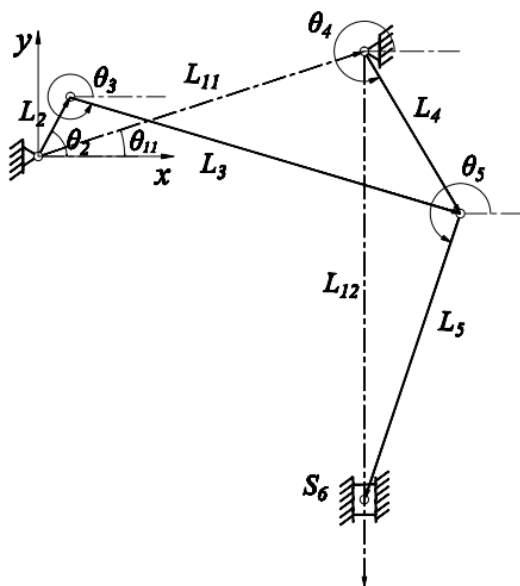


Fig 3: Kinematic analysis diagram of six-bar mechanism

As shown in figure 3, the length of the crank 2 of the six-bar mechanism is expressed as  $L_2$ , the vector of the crank 2 is expressed as  $\vec{L}_2$ , the vector angle, which is measured between the vector of the rod and the positive direction of the X axis along the counter clockwise direction, is expressed as  $\theta_2$ . The rest members of the mechanism are expressed as the same way. Since the vector of the members can form a closed polygon, such as  $\vec{L}_{11} - \vec{L}_2 - \vec{L}_4 - \vec{L}_5$  and  $\vec{L}_4 - \vec{L}_5 - \vec{L}_{12} - \vec{S}_6$ , the sum of two vectors in a closed polygon must be equal to each other. Then the equation set can be written as

$$\begin{cases} \vec{L}_2 + \vec{L}_3 = \vec{L}_{11} + \vec{L}_4 \\ \vec{L}_4 + \vec{L}_5 + \vec{S}_6 = \vec{L}_{12} \end{cases} \quad (1)$$

Equation (1) is the closed vector position equation of the six-bar mechanism model. In this model, the motion law of the crank 2 and the length of each member are known. Therefore, three unknown direction angles  $\theta_3$ ,  $\theta_4$ ,  $\theta_5$  and the displacement of the slider  $S_6$  can be obtained by equation (1). The equation (1) can be written in polar form as

$$\begin{cases} L_2 e^{i\theta_2} + L_3 e^{i\theta_3} = L_{11} e^{i\theta_{11}} + L_4 e^{i\theta_4} \\ L_4 e^{i\theta_4} + L_5 e^{i\theta_5} + S_6 e^{i\theta_{12}} = L_{12} e^{i\theta_{12}} \end{cases} \quad (2)$$

Putting Euler's formula  $e^{i\theta} = \cos\theta + i\sin\theta$  into the equation (2), we can obtain

$$\begin{cases} L_2 \cos\theta_2 + L_3 \cos\theta_3 = L_{11} \cos\theta_{11} + L_4 \cos\theta_4 \\ L_2 \sin\theta_2 + L_3 \sin\theta_3 = L_{11} \sin\theta_{11} + L_4 \sin\theta_4 \\ L_4 \cos\theta_4 + L_5 \cos\theta_5 = 0 \\ L_4 \sin\theta_4 + L_5 \sin\theta_5 + S_6 = L_{12} \end{cases} \quad (3)$$

From the equation (3), we can get

$$\begin{aligned} L_{11}^2 + L_2^2 + L_4^2 - 2L_{11}L_2 \cos(\theta_2 - \theta_{11}) + (2L_{11}L_4 \cos\theta_{11} - \\ 2L_2L_4 \cos\theta_2) \cos\theta_4 + (2L_{11}L_4 \sin\theta_{11} - 2L_2L_4 \sin\theta_2) \sin\theta_4 = L_{12}^2 \end{aligned} \quad (4)$$

Equation (4) can be simplified as

$$A \sin\theta_4 + B \cos\theta_4 + C = 0 \quad (5)$$

Where,  $A = 2L_{11}L_4 \cos\theta_{11} - 2L_2L_4 \cos\theta_2$

$$B = 2L_{11}L_4 \sin\theta_{11} - 2L_2L_4 \sin\theta_2$$

$$C = L_{11}^2 + L_2^2 + L_4^2 - L_{12}^2 - 2L_{11}L_2 \cos(\theta_2 - \theta_{11})$$

By applying trigonometric function formula, the equation (5) can be transformed into

$$2A \sin \frac{\theta_4}{2} \cos \frac{\theta_4}{2} + B \left( \cos^2 \frac{\theta_4}{2} - \sin^2 \frac{\theta_4}{2} \right) + C \left( \sin^2 \frac{\theta_4}{2} + \cos^2 \frac{\theta_4}{2} \right) = 0 \quad (6)$$

From the equation (6), we can obtain

$$(B - C) \tan^2 \frac{\theta_4}{2} - 2A \tan \frac{\theta_4}{2} - (B + C) = 0 \quad (7)$$

Therefore,  $\tan \frac{\theta_4}{2}$  and  $\theta_4$  are expressed as

$$\tan \frac{\theta_4}{2} = \frac{A \pm \sqrt{A^2 + B^2 - C^2}}{B - C} \quad (8)$$

$$\theta_4 = 2\arctan \frac{A - \sqrt{A^2 + B^2 - C^2}}{B - C} \quad (9)$$

Taking  $\theta_4$  into equation (3),  $\theta_3$ ,  $\theta_5$  and  $S_6$  can be given by

$$\theta_3 = \arccos \left( \frac{L_{11} \cos \theta_{11} + L_4 \cos \theta_4 - L_2 \cos \theta_2}{L_3} \right) \quad (10)$$

$$\theta_5 = \arccos \left( \frac{-L_4 \cos \theta_4}{L_5} \right) \quad (11)$$

$$S_6 = L_{12} - L_4 \sin \theta_4 - L_5 \sin \theta_5 \quad (12)$$

### 2.3 Velocity model of the mechanism

Taking one derivative of equation (3) with respect to time the velocity model of the six-bar mechanism can be written as

$$\begin{cases} -\omega_3 L_3 \sin \theta_3 + \omega_4 L_4 \sin \theta_4 = \omega_2 L_2 \sin \theta_2 \\ \omega_3 L_3 \cos \theta_3 - \omega_4 L_4 \cos \theta_4 = -\omega_2 L_2 \cos \theta_2 \\ -\omega_4 L_4 \sin \theta_4 - \omega_5 L_5 \sin \theta_5 = 0 \\ \omega_4 L_4 \cos \theta_4 + \omega_5 L_5 \cos \theta_5 + V_6 = 0 \end{cases} \quad (13)$$

From equation (13), we can obtain

$$L_2 \omega_2 \sin(\theta_4 - \theta_2) = L_3 \omega_3 \sin(\theta_3 - \theta_4) \quad (14)$$

So  $\omega_3$  can be given by

$$\omega_3 = \frac{L_2 \omega_2 \sin(\theta_4 - \theta_2)}{L_3 \sin(\theta_3 - \theta_4)} \quad (15)$$

Taking equation (15) into equation (13),  $\omega_3$ ,  $\omega_5$  and  $V_6$  can be written as

$$\omega_4 = \frac{L_2 \omega_2 \sin(\theta_2 - \theta_3)}{L_4 \sin(\theta_4 - \theta_3)} \quad (16)$$

$$\omega_5 = \frac{-L_4 \omega_4 \sin \theta_4}{L_5 \sin \theta_5} \quad (17)$$

$$V_6 = -L_4 \omega_4 \cos \theta_4 - L_5 \omega_5 \cos \theta_5 \quad (18)$$

### 2.4 Acceleration model of the mechanism

Taking the second derivative of formula (3) with respect to time the acceleration model of the six-bar mechanism can be expressed as

$$\begin{cases} -L_3 \omega_3^2 \cos \theta_3 - L_4 \alpha_4 \sin \theta_4 - L_2 \omega_2^2 \cos \theta_2 - L_4 \alpha_4 \sin \theta_4 = -L_2 \omega_2^2 \cos \theta_2 - L_4 \alpha_4 \sin \theta_4 \\ -L_3 \omega_3^2 \sin \theta_3 + L_4 \alpha_4 \cos \theta_4 - L_2 \omega_2^2 \sin \theta_2 + L_4 \alpha_4 \cos \theta_4 = -L_2 \omega_2^2 \sin \theta_2 + L_4 \alpha_4 \cos \theta_4 \\ -L_4 \omega_4^2 \cos \theta_4 - L_4 \alpha_4 \sin \theta_4 - L_5 \omega_5^2 \cos \theta_5 - L_4 \alpha_4 \sin \theta_4 = 0 \\ -L_4 \omega_4^2 \sin \theta_4 + L_4 \alpha_4 \cos \theta_4 - L_5 \omega_5^2 \sin \theta_5 + L_4 \alpha_4 \cos \theta_4 + a_6 = 0 \end{cases} \quad (19)$$

Solving the equation (19), we can obtain

$$\alpha_4 = \frac{-[L_2 \omega_2^2 \cos(\theta_4 - \theta_2) + L_3 \omega_3^2 \cos(\theta_3 - \theta_4) - L_4 \omega_4^2]}{L_3 \sin(\theta_3 - \theta_4)} \quad (20)$$

$$\alpha_4 = \frac{-[L_2 \omega_2^2 \cos(\theta_3 - \theta_2) + L_4 \omega_4^2 \cos(\theta_3 - \theta_4) - L_3 \omega_3^2]}{L_4 \sin(\theta_3 - \theta_4)} \quad (21)$$

$$\alpha_5 = \frac{-L_4 \omega_4^2 \cos \theta_4 - L_4 \alpha_4 \sin \theta_4 - L_5 \omega_5^2 \cos \theta_5}{L_5 \sin \theta_5} \quad (22)$$

$$a_6 = L_4 \omega_4^2 \sin \theta_4 - L_4 \alpha_4 \cos \theta_4 + L_5 \omega_5^2 \sin \theta_5 - L_5 \alpha_5 \cos \theta_5 \quad (23)$$

## 3 Dynamics model of the six-bar mechanism

### 3.1 Generalized coordinates of the six-bar mechanism

From figure 10, crank 2 is the driving link in the single degree of freedom six-bar mechanism. When the angular displacement of crank 2 is determined, the position of the whole mechanism is also determined, and thus, the angular displacement of the crank can be taken as the generalized coordinates, that is  $q = \theta_2$ .

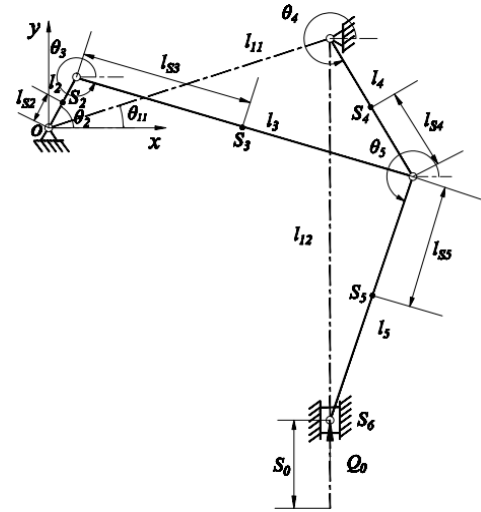


Fig 10: Dynamics analysis diagram of six-bar mechanism

The Lagrange formula for a single degree of freedom system is expressed as

$$\frac{d}{dt} \left( \frac{\partial E}{\partial \dot{q}} \right) - \frac{\partial E}{\partial q} + \frac{\partial U}{\partial q} = Q \quad (24)$$

Where,  $E$ ,  $U$ ,  $Q$ ,  $q$  are the kinetic energy, potential energy, generalized force and generalized coordinates of the system, respectively.

In order to apply the formula (24) to establish the dynamic model of the system, the system's kinetic energy, potential energy and generalized force should be listed first.

### 3.2 The Lagrange dynamic equation of the six-bar mechanism

#### 3.2.1 Kinetic energy of the six-bar mechanism

To calculate the kinetic energy of the mechanism, we must know the angular velocity and the velocity of the center of mass of each member. By kinematic analysis of the mechanism, we can get

$$\begin{cases} \theta_i = \theta_i(q) \\ x_{Si} = x_{Si}(q) \\ y_{Si} = y_{Si}(q) \end{cases} \quad (25)$$

Where  $\theta_i$  is the angular displacement of component  $i$ ,  $x_{Si}$  and

$y_{si}$  are the coordinates of the centroid of the component in the  $x$  axis and  $y$  axis.

Taking derivative of equation (25) with respect to time, the angular velocity  $\dot{\theta}_i$  of the component  $i$ , the speed of centroid  $\dot{x}_{si}$  in the  $x$  axis and  $\dot{y}_{si}$  in the  $y$  axis can be obtained as

$$\begin{cases} \dot{\theta}_i = \frac{\partial \theta_i(q)}{\partial q} \dot{q} \\ \dot{x}_{si} = \frac{\partial x_{si}(q)}{\partial q} \dot{q} \\ \dot{y}_{si} = \frac{\partial y_{si}(q)}{\partial q} \dot{q} \end{cases} \quad (26)$$

Where  $q$ ,  $\dot{q}$  is the generalized coordinates and velocity, respectively

The velocity of the center of mass  $S_i$  can be given by

$$V_{Si} = \sqrt{\dot{x}_{Si}^2 + \dot{y}_{Si}^2} \quad (27)$$

The kinetic energy of the six-bar mechanism can be expressed as

$$E = \sum_{i=2}^6 \frac{1}{2} (m_i v_{Si}^2 + J_i \dot{\theta}_i^2) \quad (28)$$

Taking equation (26), (27) into equation (28), we can obtain

$$E = \sum_{i=2}^6 \frac{1}{2} \left\{ m_i \left[ \left( \frac{\partial x_{si}}{\partial q} \right)^2 + \left( \frac{\partial y_{si}}{\partial q} \right)^2 \right] + J_i \left( \frac{\partial \theta_i}{\partial q} \right)^2 \right\} \dot{q}^2 \quad (29)$$

From equation (29), the kinetic energy of the system can be expressed as

$$E = \frac{1}{2} J_e \dot{q}^2 \quad (30)$$

Where

$$J_e = \sum_{i=2}^6 m_i \left[ \left( \frac{\partial x_{si}}{\partial q} \right)^2 + \left( \frac{\partial y_{si}}{\partial q} \right)^2 \right] + J_i \left( \frac{\partial \theta_i}{\partial q} \right)^2$$

is a function of  $q$ , and is uncorrelated with  $\dot{q}$ . In other words, the equivalent moment of inertia is related to the size of the mechanism, the moment of inertia of each member and the position  $q$  of the mechanism. And the  $J_e$  is always a positive number.

### 3.2.2 Potential energy of the six-bar mechanism

The zero potential energy position is located at the origin of the coordinate (see figure 9), the positive direction of the X axis is the direction of gravity, the potential energy of the system is written as

$$U = -m_2 g x_{s2} - m_3 g x_{s3} - m_4 g x_{s4} - m_5 g x_{s5} - m_6 g L_{11} \cos \theta_{11} \quad (31)$$

### 3.2.3 Generalized force of the six-bar mechanism

The generalized force can be determined according to the virtual work principle. For a single degree of freedom six-bar mechanism, the relationship between the virtual work  $\delta W$  of active force and the generalized virtual displacement can be given by

$$\delta W = Q \delta q \quad (32)$$

Where the coefficient  $Q$  in front of generalized virtual displacement is generalized force.

For the single degree of freedom six-bar mechanism, according to the virtual work principle, we can get

$$\delta W = Q \delta q = M_2 \delta q - Q_0 \left[ \frac{\partial (L_{12} - S_0)}{\partial q} \delta q \right] \quad (33)$$

Where,  $Q_0$  is the load applied to the slider.

From the equation (33), the generalized force of the system is given by

$$Q = M_2 + Q_0 \frac{\partial S_0}{\partial q} \quad (34)$$

Where,  $M_2$  is the torque of the motor acting on the crank,  $S_0$  is the displacement of the slider

### 3.2.4 Motion differential equation of the six-bar mechanism

Taking derivative of equation (30) with respect to  $q$  and  $\dot{q}$  respectively, we can get

$$\frac{\partial E}{\partial q} = \frac{1}{2} \dot{q}^2 \frac{\partial J_e}{\partial q} \quad (35)$$

$$\begin{cases} \frac{\partial E}{\partial \dot{q}} = J_e \dot{q} \\ \frac{d}{dt} (J_e \dot{q}) = J_e \frac{d\dot{q}}{dt} + \dot{q} \frac{\partial J_e}{\partial q} \frac{dq}{dt} = J_e \frac{d\dot{q}}{dt} + \dot{q}^2 \frac{\partial J_e}{\partial q} \end{cases} \quad (36)$$

According to the equation (31), we can get

$$\frac{\partial U}{\partial q} = -m_2 g \frac{\partial x_{s2}}{\partial q} - m_3 g \frac{\partial x_{s3}}{\partial q} - m_4 g \frac{\partial x_{s4}}{\partial q} - m_5 g \frac{\partial x_{s5}}{\partial q} - m_6 g \frac{\partial L_{11} \cos \theta_{11}}{\partial q} \quad (37)$$

The dynamic equation of the novel six-bar mechanism is expressed as

$$J_e \ddot{q} + \frac{1}{2} \frac{\partial J_e}{\partial q} \dot{q}^2 + \frac{\partial U}{\partial q} = Q \quad (38)$$

## 4. Example of kinematic and force analysis of six-bar mechanism

### 4.1 System parameters of the six-bar mechanism

System parameters of the six-bar mechanism are shown in table 1.

**Table 1:** System parameters of the six-bar mechanism

Design parameters	parameter values
Distance between rotation center of crank 2 and rotation center of rocking-bar 4 $L_{11} / mm$	434
Distance from frames to bottom dead centre of the sliding block 6 $L_{12} / mm$	650
Length of the crank 2 $L_2 / mm$	202
Length of the linkage 3 $L_3 / mm$	540
Length of the rocking-bar 4 $L_4 / mm$	250
Length of the linkage 5 $L_5 / mm$	400
Inclination angle of the frame $\theta_{11} / (^{\circ})$	11
Initial angle of crank 2 $\theta_2 / (^{\circ})$	160.24
Quality of the crank 2 $m_2 / kg$	0.037
Rotational speed of the crank 2 $\omega_2 / (^{\circ} / s)$	120
Quality of the linkage 3 $m_3 / kg$	0.213
Quality of the rocking-bar 4 $m_4 / kg$	0.100
Quality of the linkage 5 $m_5 / kg$	0.158
Quality of the sliding block 6 $m_6 / kg$	0.139
Rotational inertia of the linkage 3 $J_{3c} (kg / m^2)$	$5.27 \times 10^{-3}$
Rotational inertia of the rocking-bar 4 $J_{4c} (kg / m^2)$	$5.42 \times 10^{-4}$
Rotational inertia of the linkage 5 $J_{5c} (kg / m^2)$	$2.17 \times 10^{-3}$

**4.2 Example of kinematic analysis**

When the crank 2 of six-bar mechanism runs three cycles, the numerical calculation of the displacement of the slider by Matlab and the virtual prototype simulation of the displacement of the slider by ADAMS are shown in figure 11, the numerical calculation of the velocity of the slider by

Matlab and the virtual prototype simulation of the velocity of the slider by ADAMS are shown in figure 12, the numerical calculation of the acceleration of the slider by Matlab and the virtual prototype simulation of the acceleration of the slider by ADAMS are shown in figure 13.

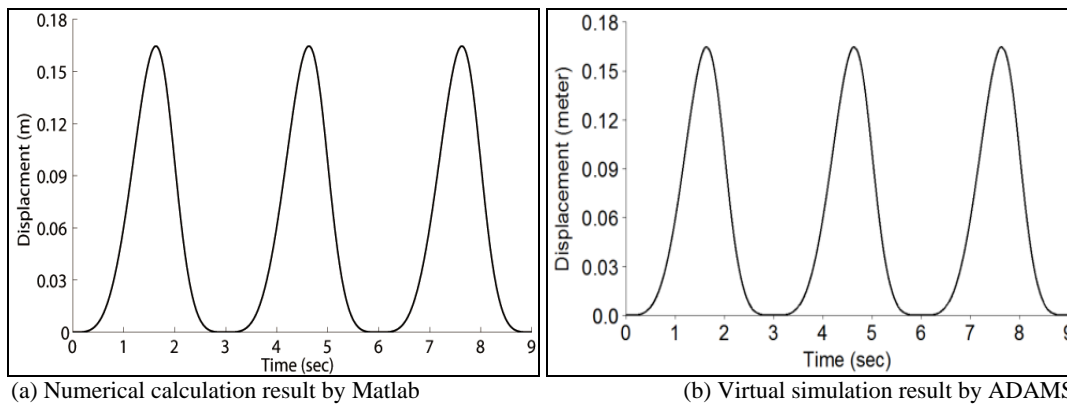


**Fig 11:** The displacement of six-bar mechanism's slider

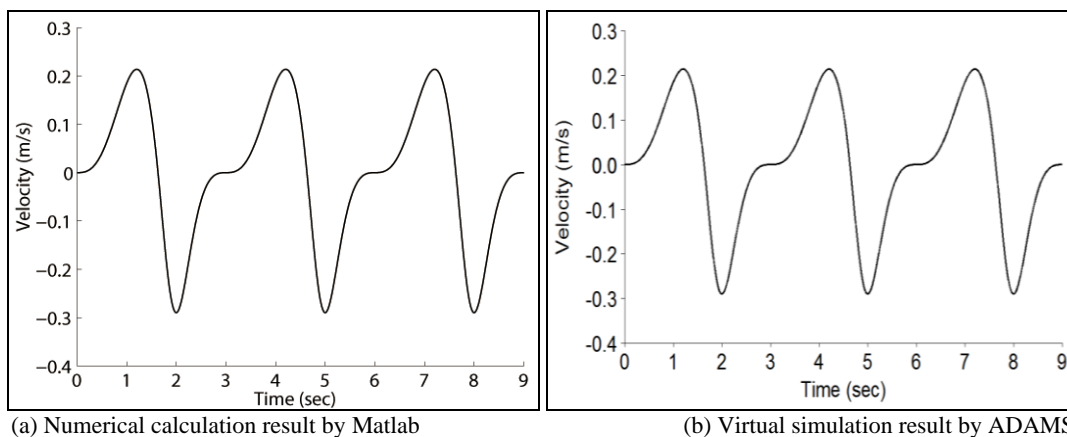


**Fig 12:** The velocity of six-bar mechanism's slider

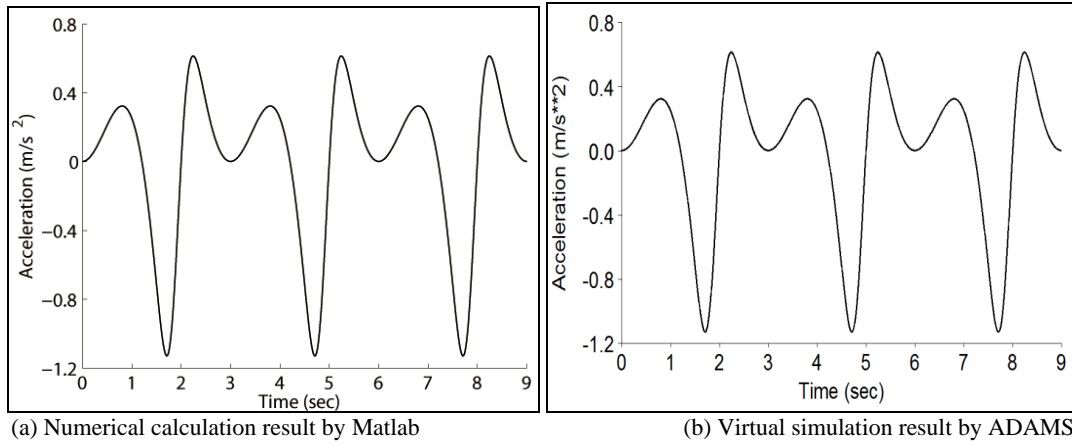


Fig 13: The acceleration of six-bar mechanism's slider

From figure 11 to figure 13, the trend and the peak value of the displacement curves, velocity curves, and acceleration curves are basically similar; the maximum error of the displacement, which occurs in 1.63s, is 0.0002m; the maximum error of the velocity, which occurs in 1.21s, is 0.0001m/s; the maximum error of the acceleration, which occurs in 1.71s, is 0.0001m/s<sup>2</sup>.

4.3 Example of dynamics analysis

When the slider 6 of six-bar mechanism moves with no-

load, that is  $F_r = 0$ , The numerical calculation of the driving torque of the crank by Matlab and the virtual prototype simulation of the driving torque of the crank by ADAMS are shown in figure 19. When the slider 6 of six-bar mechanism runs with load, that is  $F_r = 100kN$ , The numerical calculation of the driving torque of the crank by Matlab and the virtual prototype simulation of the driving torque of the crank by ADAMS are shown in figure 20.

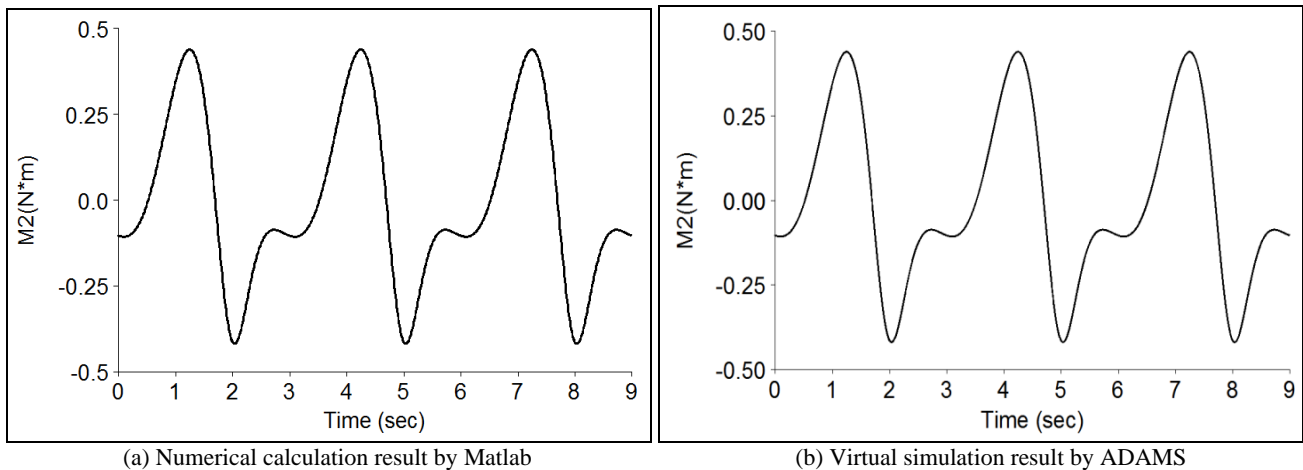


Fig 19: The driving torque of six-bar mechanism when the slider with no load

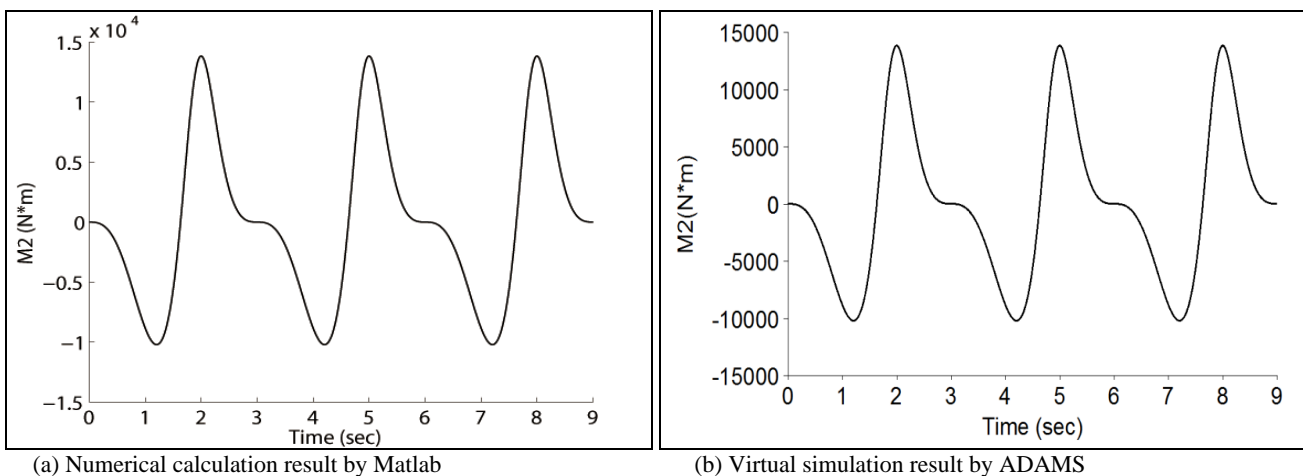


Fig 20: The driving torque of six-bar mechanism when the slider with load

From figure 19 to figure 20, the numerical calculation results obtained by Matlab is almost completely consistent

with the virtual simulation results obtained by ADAMS; When the slider 6 of six-bar mechanism runs with load, the

maximum error of the driving torque, which occurs in 2.0s, is 1.018Nm; When the slider 6 of six-bar mechanism runs with no-load, the maximum error of the driving torque, which occurs in 1.25s, is 0.0254Nm.

### 5. Conclusion

1. The kinematic model of a six-bar linkage mechanism is established by using the complex vector method, the kinematic analysis including slider position, slider velocity, slider acceleration is realized and verified.
2. The dynamic model of the six-bar mechanism is established by using the Lagrange Method. The driving torque on crank is solved out and verified.
3. This study provide theoretical basis for kinematic analysis, force analysis and structure design of the six-bar mechanism, and suggest a way of analytical modeling for other multi-link mechanism.

### 6. Acknowledgments

This research is supported by Shandong key research and development public welfare program (GrantNo. 2019GGX104011), and Natural Science Foundation of Shandong Province (GrantNo.ZR2017MEE066).

### 7. References

1. Du R, Guo WZ. The Design of a new metal forming press with controllable mechanism [J]. *Journal of Mechanical Design*. 2003; 125(3):582-592.
2. Meng CF, Ce- Zhang, Lu YH. Optimal design and control of a novel press with an extra motor [J]. *Mechanism & Machine Theory*. 2004; 39(8):811-818.
3. Zhou Y. Type synthesis and optimization of main driving mechanism for servo-punch press [J]. *Journal of Mechanical Engineering*. 2015; 51(11):1-7.
4. Tso PL. Optimal design of a hybrid-driven servo press and experimental verification [J]. *Journal of Mechanical Design*. 2010; 132(3):0345031-0345034.
5. Jih-Lian Ha, Rong-Fong Fung, Kun-Yung Chen, Shao-Chien Hsien. Dynamic modeling and identification of a slider-crank mechanism [J]. *Journal of Sound and Vibration*. 2006; (289):1019-1044.
6. Li H, Zhang Y, Zheng H. Dynamics modeling and simulation of a new nine-bar press with hybrid-driven mechanism [J]. *Journal of Mechanical Science & Technology*. 2009; 22(12):2436-2444.
7. He K, Li W, Du R. Dynamic modeling with kineto-static method and experiment validation of a novel controllable mechanical metal forming press. [J] *International Journal of Manufacturing Research*. 2006; 1(3):354-378.
8. Lee HJ. Dynamics and probabilistic fatigue analysis schemes for high-speed press machines [J] *Computer and structures*. 1994; (1):11-19.
9. Barker CR, Tso PL. Characteristic surfaces for three position function generation with planar four bar mechanisms. [J]. *American Society of Mechanical Engineers Design Engineering Division De*. 1987; 111(1):135-142.
10. Lu Xinjian, Zhu Sihong, He Guangjun. Kinematic analysis of multi-link high-speed presses [J]. *China Mechanical Engineering*. 2011; 22(11):1297-1301.
11. Gong Jinliang, Wang Xiaoming, Huang Fengang. Dynamic performances analysis of hybrid press based on dependent generalized coordinates [J]. *Proceedings of the Institution of Mechanical Engineers, Part C: Journal of Mechanical Engineering Science*. 2015; 229(12):2187-2194.
12. Neumann M, Hahn H. Computer simulation and dynamic analysis of a mechanical press based on different engineer models [J]. *Mathematics & Computers in Simulation*. 1998; 46(5-6):559-574.
13. Tso PL, Liang KC. A nine-bar linkage for mechanical forming presses [J]. *International Journal of Machine Tools & Manufacture*. 2002; 42(1):139-145.
14. Kireççi A, Dulger LC. A study on a hybrid actuator [J]. *Mechanism & Machine Theory*. 2000; 35(8):1141-1149.
15. Dulger LC, Kireççi A, Topalbekiroglu M. Modeling and simulation of a hybrid actuator [J]. *Mechanism & Machine Theory*. 2003; 38(5):395-407.
16. Xiao-Dong YE, Ya-Yin HE. Study on motion characteristics of drawing press outer slide mechanisms based on the virtual prototype [J]. *Journal of Machine Design*. 2013; 30(7):38-41.
17. Seth B, Vaddi SS. Programmable function generators—I: base five-bar mechanism [J]. *Mechanism & Machine Theory*, 2003, 38(4):321-330.
18. Sesha Sai Vaddi, Bhartendu Seth. Programmable function generators—II: seven-bar translatory-output mechanism [J]. *Mechanism & Machine Theory*. 2003; 38(4):331-343.
19. Hui LI, Zhang C. Research on the feasibility of hybrid-driven mechanical press [J]. *Mechanical Science & Technology*. 2004; 23(10):1253-1256.
20. Jin XX. Research on mechanism synthesis of seven-link hybrid-driven servo press [J]. *Forging & Stamping Technology*. 2013; 38(3):107-110.